Research on Cumulative Damage Evaluation Method for Structural Impact on Airborne Armored Vehicle in Landing Process

Xinhua Fu[1,*], Yong Lu[2], Jun Wang[1] and Xueyang Chen[1]

[1]Airborne Training Center, Guilin, Guangxi, 541003, China.
[2]Scholl of Computer Science, University of Electronic Science and Technology of China, Zhongshan Institute, Zhongshan, 528402, China.
*Email[1]: fuxinhua_003@163.com

Abstract. Since it was very costly and complicated to analyze cumulative damage caused by structural impact on airborne armored vehicle in landing process using real equipment airdrop test, finite element method(FEM) was taken to build a finite element(FE) model of airborne armored vehicle and airbag system to simulate the landing impact process of airborne armored vehicle. In combination with Lemaitre Damage Model and the damage evolution law of materials, the cumulative damage caused by structural impact of vehicle was calculated. The cumulative damage of structure of airborne armored vehicle in multiple landing processes was assessed, results of which were expected to provide theoretical guidance for the operational use and maintenance of airborne armored vehicle.

1. Introduction

Impact load was one of the main factors causing structural damage to airborne armored vehicle in the landing process. For airborne armored vehicle with thin-shelled and complicated structure, the impact produced in the landing and buffering period would cause plastic deformation and structural damage to its structure partially. Such structural damage, however, can be transmitted and cumulated due to the repeatable airdrop characteristic of airborne armored vehicle[1]. Undoubtedly, cumulative damage to the body of airborne armored vehicle would greatly affect its technical conditions during the subsequent service. At present, two methods are mainly adopted in researches on the cumulative damage caused by structural impact on airborne armored vehicle under the condition of landing impact, namely, real equipment airdrop test and numerical simulation. Influenced by factors such as climate and ground environment, the landing conditions for airborne armored vehicle varied widely along with the challenge of prediction. As a result, a huge investment in manpower, material and financial resources would be required to conduct real equipment airdrop tests under multiple landing conditions. At the beginning of developing and finalizing airborne armored vehicle, real equipment airdrop tests had been conducted, but the test data was too limited to meet research requirements for cumulative damage from structural impact[1-2]. In recent years, the development of computer technology and the theory of finite element have provided a new approach for researching the cumulative damage caused by structural impact on airborne armored vehicle in the landing process. With the method of finite element, a finite element model of airborne armored vehicle and airbag system was built, and a non-linear finite-element model was used to simulate the process of landing impact on airborne armored vehicle. Meanwhile, in combination with Lemaitre Damage Model and the damage evolution law of materials, the cumulative damage from structural impact was calculated, and an analysis was conducted toward the cumulative damage evaluation for the structure of airborne armored vehicle

during repeated landing, so as to provide theoretical guidance for the operational use and maintenance of airborne armored vehicle.

2. Finite Element Analysis Model

2.1. Lemaitre Damage Model

Based on the theory of energy damage, Lemaitre presented a model for evaluating the structural damage under significant plastic deformation, which is presented as follows [3]:

$$D = D_R \frac{\varepsilon_p \varepsilon_t - \varepsilon_D}{\varepsilon_R - \varepsilon_D}$$

Where, D, D_R and ε_p represent damage variable, damage limit value and cumulative plastic strain respectively, ε_D and ε_R correspond to plastic strain of damage threshold value and damage limit value, and ε_t reflects the influence of triaxial stress ratio on material damage, which is called triaxial stress factor.

$$\varepsilon_t = \frac{2}{3}(1+v) + 3(1-2v)\left(\frac{\sigma_H}{\sigma_{eq}}\right)^2$$

Under uniaxial stress, $\sigma_H = \sigma / 3$, $\sigma_{eq} = \sigma$, ε_t=1.

In Lemaitre Damage Model, the damage model parameters ε_D, ε_R and D_R can be obtained by measuring the variation of elasticity modulus of materials.

2.2. Analysis Process

The process of analyzing the cumulative damage caused by structural impact on airborne armored vehicle in landing process is shown in Figure 1.

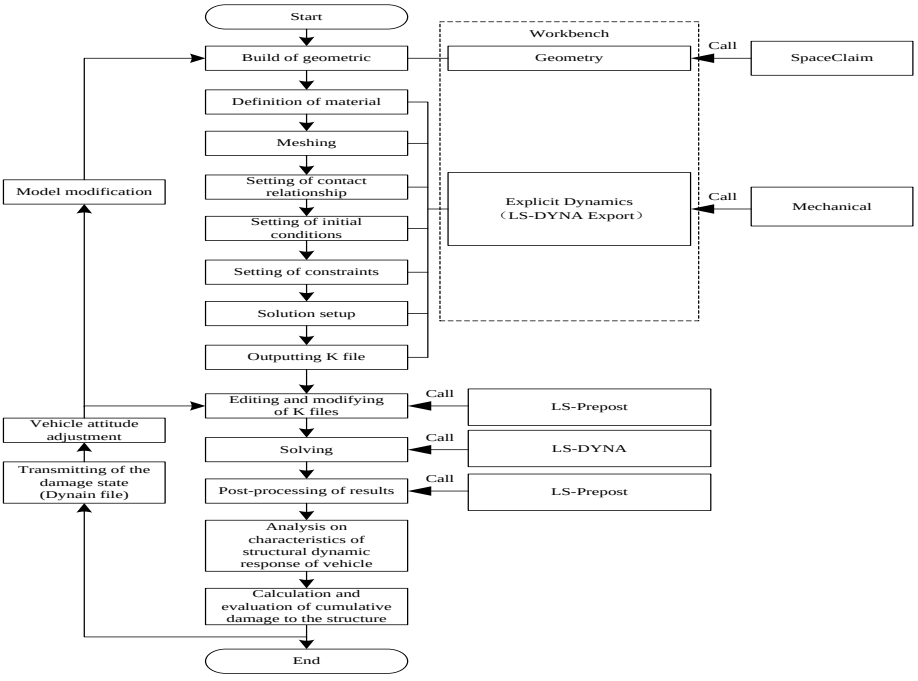

Figure 1. Process of Analyzing the Cumulative Damage caused by Structural impact on Airborne Armored Vehicle in Landing Process

(1) The establishment of File K for model analysis. Based on the software of ANSYS, the simulation and analysis model for the landing and buffering process of airborne armored vehicle was built in accordance with steps such as geometric modeling, material definition, meshing, contact relation setting, initial condition setting, constraints setting, solution setup, File K output, and File K edition and modification. Mesh refinement was conducted towards the parts and components such as the main support structure of vehicle body and the engine support. Johnson-cook Model was selected as the material model of vehicle body[4]. The established finite element model of airborne armored vehicle and airbag system is shown in Figure 2.

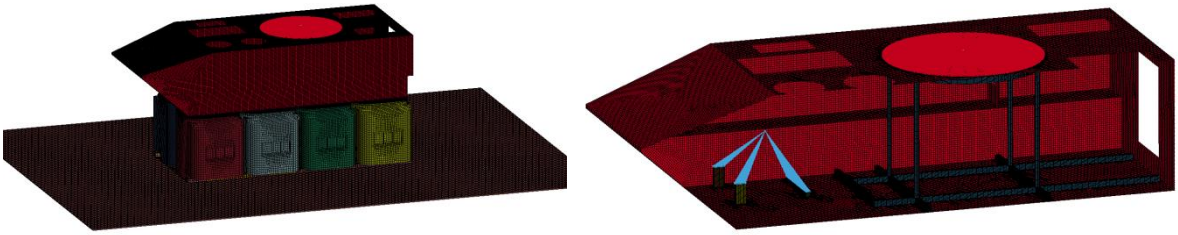

Figure 2. Finite Element Model of Airborne Armored Vehicle and Airbag System

(2) Solving of File K. LS-DYNA solver was called to solve the analysis model, that is, the modified File K.

(3) Viewing of simulation results. The output data obtained by simulation calculation was imported into LS-Prepost to view the results data and related curves, such as stress contours, stress change curve, and plastic strain contours.

(4) Analysis on characteristics of structural dynamic response of vehicle. Based on the simulation data, characteristics of structural dynamic response of vehicle in the landing process this time were analyzed.

(5) Transmitting of the damage state. The damage distribution of vehicle under the *i*-th landing impact was used as the initial condition of the (*i*+1)-th calculation, that is, file Dynain with the stress-strain data output from the *i*-th simulating calculation was imported into file K, the analysis model established in step (1), and the vehicle attitude was adjusted simultaneously.

(6) Calculation and evaluation of cumulative damage to the structure. Step (2) to (4) were repeated to obtain characteristics of structural dynamic response of vehicle in the (*i*+1)-th landing process. In combination with Lemaitre Damage Model and the damage evolution law of materials, cumulative damage to the structure was calculated.

(7) Similarly, by repeating step (5) to (6), cumulative damage to the structure of vehicle in the (*i*+2)-th landing process could be figured out via simulating calculation, thus obtaining the cumulative damage to the structure of vehicle under repeated airdrop, the process of which continued until the destroying threshold of components was met.

3. Simulating Calculation of Cumulative Damage

3.1. Simulation Results

Based on the established finite element model of airborne armored vehicle and airbag system, simulating calculation was carried out towards the landing and buffering process of airborne armored vehicle under typical airdrop conditions, so as to obtain the simulation results such as stress contours, stress change curve, and plastic strain contours. In combination with Lemaitre Damage Model and the damage evolution law of materials, the cumulative damage from structural impact was calculated, and an analysis was conducted towards the cumulative damage evaluation for the structure of airborne armored vehicle under repeated airdrop. When the vertical landing speed is 8m/s over a plain, the value of cumulative damage to typical structural parts of airborne armored vehicle in the landing process is shown in Table 1, and when the speed is 9m/s, the value is shown in Table 2, where the italic number indicates that the element number corresponding to the maximum stress value is

different from that corresponding to the maximum plastic strain on a certain part or component. If a certain component contains two element numbers, it suggests that the position of maximum stress is changed between the two consecutive times of airdrop.

Table 1. Cumulative Damage to Structure of Typical Vehicle Parts at the Vertical Landing Speed of 8m/s

Time of Airdrop	Typical Damage Part	Specific element number	Max stress value (MPa)	Max plastic stress (%)	Damage Value D	Variation D_{i+1}-D_i
The 1st time	Baseboard of armor plate	361583	216.88	0	0	0
	Bottom of the left upright in the front of vehicle	202515	304.95	0	0	0
	Bottom of the right upright in the front of vehicle	202183	348.21	0	0	0
	Bottom of the left upright at the back of vehicle	201906	320.58	0	0	0
	Bottom of the right upright at the back of vehicle	202330	361.42	0	0	0
	Bottom of the support at the back of engine	265729	137.14	0	0	0
	Bottom of the left support in the front of engine	265730	185.02	0	0	0
	Bottom of the right support in the front of engine	268979	177.47	0	0	0
The 2nd time	Baseboard of armor plate	361583	233.71	0	0	0
	Bottom of the left upright in the front of vehicle	202515	351.61	0	0	0
	Bottom of the right upright in the front of vehicle	202183	394.39	0	0	0
	Bottom of the left upright at the back of vehicle	201906	361.73	0	0	0
	Bottom of the right upright at the back of vehicle	202330	395.20	0	0	0
	Bottom of the support at the back of engine	265729	233.54	0	0	0
	Bottom of the left support in the front of engine	265730	211.85	0	0	0
	Bottom of the right support in the front of engine	268979	198.50	0	0	0
The 3rd time	Baseboard of armor plate	361583	223.85	0	0	0
	Bottom of the left upright in the front of vehicle	202515	331.76	0	0	0
	Bottom of the right upright in the front of vehicle	202183	398.65	0	0	0
	Bottom of the left upright at the back of vehicle	201906	338.29	0	0	0
	Bottom of the right upright at the back of vehicle	202330	374.89	0	0	0
	Bottom of the support at the back of engine	265729	200.02	0	0	0
	Bottom of the left support in the front of engine	265730	172.75	0	0	0
	Bottom of the right support in the front of engine	268979	268.01	0	0	0
The 4th time	Baseboard of armor plate	361583	180.25	0	0	0
	Bottom of the left upright in the front of vehicle	202515	304.23	0	0	0
	Bottom of the right upright in the front of vehicle	202183	325.80	0	0	0
	Bottom of the left upright at the back of vehicle	201906	296.96	0	0	0
	Bottom of the right upright at the back of vehicle	202330	306.15	0	0	0
	Bottom of the support at the back of engine	265729	224.54	0	0	0
	Bottom of the left support in the front of engine	265730	172.08	0	0	0
	Bottom of the right support in the front of engine	268979	192.31	0	0	0

Table 2. Cumulative Damage to Structure of Typical Vehicle Parts at the Vertical Landing Speed of 9m/s

Time of Airdrop	Typical Damage Part	Specific element number	Max stress value (MPa)	Max plastic stress (%)	Damage Value D	Variation D_{i+1}-D_i
The 1st time	Baseboard of armor plate	320806	487.50	0.46	0.017	-
	Bottom of the left upright in the front of vehicle	143924	513.52	1.50	0.055	-
	Bottom of the right upright in the front of vehicle	202183	518.64	0.92	0.034	-
	Bottom of the left upright at the back of vehicle	201906	522.67	0.97	0.035	-
	Bottom of the right upright at the back of vehicle	202330	525.42	1.01	0.037	-
		150147	458.97	0.03	0.001	
	Bottom of the support at the back of engine	265729	459.91	0.06	0.002	-
	Bottom of the left support in the front of engine	265730	497.84	0.61	0.022	-
	Bottom of the right support in the front of engine	268979	513.66	1.43	0.052	
The 2nd time	Baseboard of armor plate	320806	490.19	0.77	0.028	0.011
		289279	435.66	0.89	0.032	-
	Bottom of the left upright in the front of vehicle	143924	516.49	1.75	0.064	0.009
	Bottom of the right upright in the front of vehicle	202183	496.88	1.07	0.039	0.005
		137123	587.77	3.90	0.142	-
	Bottom of the left upright at the back of vehicle	201906	501.46	1.25	0.046	0.011
		137693	594.41	4.04	0.147	-
	Bottom of the right upright at the back of vehicle	202330	493.77	1.06	0.039	0.002
		150147	582.65	3.29	0.120	0.119
	Bottom of the support at the back of engine	265729	459.31	0.06	0.002	0
	Bottom of the left support in the front of engine	265730	510.94	1.10	0.040	0.018
	Bottom of the right support in the front of engine	268979	556.57	2.79	0.102	0.050
The 3rd time	Baseboard of armor plate	289279	538.61	2.55	0.093	0.061
	Bottom of the left upright in the front of vehicle	143924	614.84	4.59	0.167	0.103
	Bottom of the right upright in the front of vehicle	137123	695.77	6.20	0.226	0.084
	Bottom of the left upright at the back of vehicle	137693	683.89	5.46	0.199	0.052
	Bottom of the right upright at the back of vehicle	150147	756.34	7.25	0.264	0.144
	Bottom of the support at the back of engine	265729	478.95	0.36	0.013	0.011
	Bottom of the left support in the front of engine	265730	495.98	1.12	0.041	0.001
		265734	509.67	1.41	0.051	-
	Bottom of the support at the back of engine	268979	590.92	3.68	0.134	0.032
The 4th time	Baseboard of armor plate	289279	647.50	4.79	0.175	0.082
	Bottom of the left upright in the front of vehicle	143924	402.77	4.59	0.167	0
		143950	491.45	3.36	0.123	-
	Bottom of the right upright in the front of vehicle	137123	765.06	7.90	0.288	0.062
		137085	791.46	8.17	0.298	-
	Bottom of the left upright at the back of vehicle	137693	857.54	10.77	0.393	0.194
		137732	899.81	11.16	0.407	-
	Bottom of the right upright at the back of vehicle	150147	889.26	11.35	0.414	0.150
		150185	939.92	11.90	0.434	-
	Bottom of the support at the back of engine	265729	539.94	2.22	0.081	0.068
	Bottom of the left support in the front of engine	265734	556.19	2.84	0.103	0.052
	Bottom of the right support in the front of engine	268979	611.90	4.60	0.168	0.034

3.2. Result Analysis

(1) In case of repeated landing under normal conditions, that is, when the vertical landing speed was lower than 8m/s over a plain, the structural stress of vehicle would not exceed the yield limit of materials and no damage would be caused to vehicle structure, which implies that it was safe for airborne armored vehicle to implement repeated airdrop under normal conditions.

(2) When the vertical landing speed of vehicle was 9m/s, plastic strain would arise in vehicle structure, with the plastic strain contours of the whole vehicle structure shown in Figure 3, from which it could be seen that the majority of structural damages of the whole vehicle were subtle. Major

damages mainly concentrated around the root of the bottom of the four turret uprights (four uprights of the main support of vehicle body) and around the front-left vertex of the front-right engine support. The value of plastic strain on the left root of the bottom of front-left upright of the main vehicle support was 5.5%, and the value of plastic strain on the front-right vertex of the bottom of front-right engine support was 5.2%. Therefore, it could be said that the whole vehicle was relatively reasonable in structural design with full consideration of the huge load on parts such as the upright and the engine support where counter measures had been reinforced correspondingly. In consideration of increasing the strength of vehicle body and its impact resistance, it is recommended that the bottom of front-left upright and that of front-right engine support should be furthered reinforced.

(3) In repeated landing of airborne armored vehicle at a speed of 9m/s, by comparing the simulation results of repeated airdrop thereof, it could be seen that the distribution law of stress and plastic strain of the whole vehicle structure was similar, and with the increase of airdrop times, the maximum stress value, maximum plastic strain and damage value of the vehicle would all gradually rise, presenting a distinct accumulative effect of plastic strain. When airdrop was conducted for the fourth time, large plastic strain would occur to vehicle structure, with partial positions exceeding the plastic strain corresponding to the limit value of material damage and the damage value of the bottom of right upright in the front of vehicle and that of the left upright at the back of vehicle exceeding the secure threshold. It indicates that three times of airdrop could be executed at most for airborne armored vehicle at the vertical landing speed of 9m/s. Seen from the contours of effective plastic strain of whole vehicle structure in the 4th airdrop (Figure 4), the structure of vehicle had been severely deformed, which had affected the normal use of airborne armored vehicle. Therefore, the mission of airdrop failed.

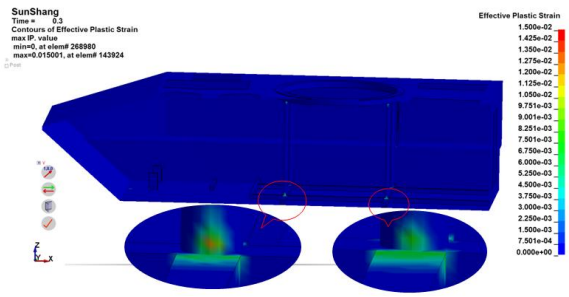

Figure 3. Plastic Strain Contours of the Whole Vehicle Structure at the Vertical Landing Speed of 9m/s for the First Time

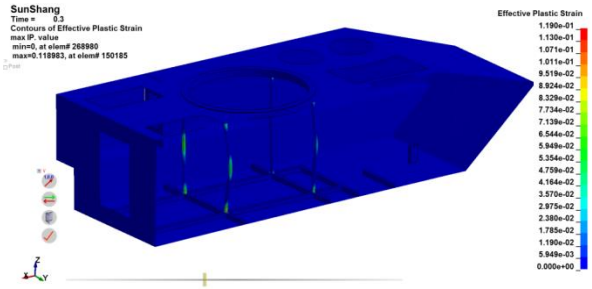

Figure 4. Plastic Strain Contours of the Whole Vehicle Structure at the Vertical Landing Speed of 9m/s for the Fourth Time

(4) In repeated landing of airborne armored vehicle at a speed of 9m/s, by comparing the stress change curve of the 143924th element which is at the bottom of the left upright in the front of vehicle (Figure 5), the stress change curve of the 150147th element which is at the bottom of the right upright at the back of vehicle (Figure 6), and the stress change curve of the 268979th element which is at the bottom of the right support in the front of engine (Figure7) in previous two times of airdrop, the stress state of these positions had changed already due to plastic strain in the first time of airdrop, while the existence of residual stress had led to initial stress and strain already at the beginning of the 2nd simulation of landing. In the front section of the curves, that is, before the landing of airborne armored vehicle, the stress change curve in the 1st airdrop was on monotonically increase, and the stress rapidly increased when the vehicle was about to touch the ground, making the curve relatively steep. While the stress change curve in the 2nd airdrop presents an oscillating phenomenon, but in the same way, the stress increased rapidly when the vehicle was about to touch the ground, making the curve relatively steep. The reason for oscillation of the stress change curve in the 2nd airdrop was that residual stress existed in the 1st airdrop. In the rail section of the curve, that is, after the landing of the vehicle, the stress change curves in the two times of airdrop both presented oscillation, with the impact

energy converted into structural deformation, where elastic deformation existed partially and the energy it stored could be dispersed through vibration.

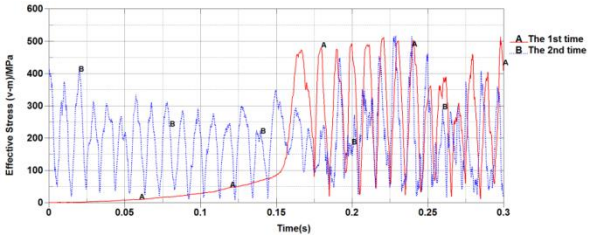

Figure 5. Comparison of the Stress Change Curve of the 143924th Element in Previous Two Times of Airdrop

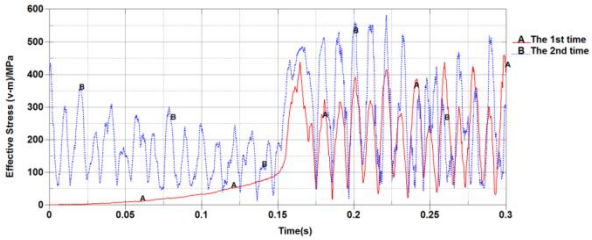

Figure 6. Comparison of the Stress Change Curve of the 150147th Element in Previous Two Times of Airdrop

(5) In repeated landing of airborne armored vehicle at a speed of 9m/s, by comparing the plastic strain change curve of the 143924th element at the bottom of the left upright in the front of vehicle (Figure 8), the plastic strain change curve of the 150147th element at the bottom of the right upright at the back of vehicle (Figure 9), and the plastic strain change curve of the 268979th element at the bottom of the right support in the front of engine (Figure10) in four times of airdrop, it could be found that the plastic strain value in the same position was gradually cumulated by a certain trend rather than remain unchanged, that is to say, the damage value was cumulated gradually. In each time of airdrop, the stress of the whole vehicle structure was usually the maximum when the vehicle was about to touch the ground. At this moment, a sudden increase would happen to the plastic strain. However, the increase of plastic strain value did not follow the linear law each time, which indicates that the damage value did not always increase linearly.

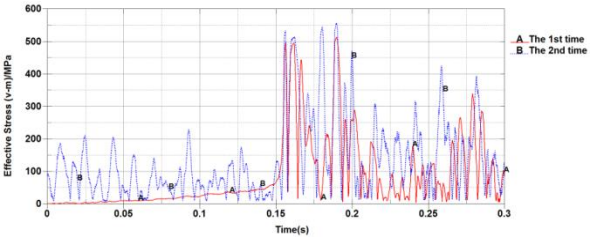

Figure 7. Comparison of the Stress Change Curve of the 268979th Element in Previous Two Times of Airdrop

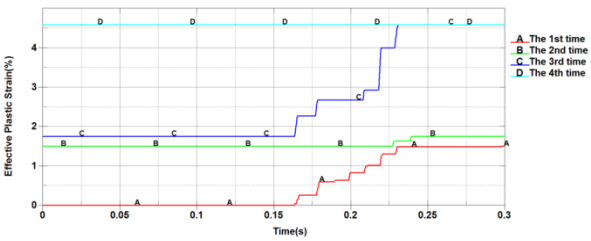

Figure 8. Comparison of the Plastic Strain Change Curve of the 143924th Element in Four Times of Airdrop

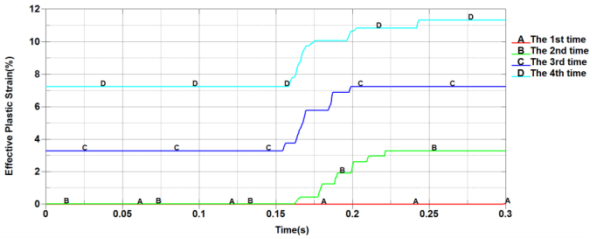

Figure 9. Comparison of the Plastic Strain Change Curve of the 150147th Element in Four Times of Airdrop

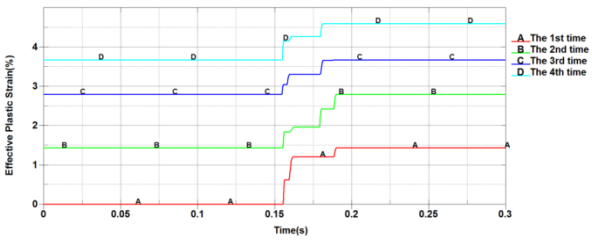

Figure 10. Comparison of the Plastic Strain Change Curve of the 268979th Element in Four Times of Airdrop

4. Conclusions

With finite element method, a finite element model of airborne armored vehicle and airbag system was established to simulate the landing process of airborne armored vehicle. Through simulating

calculation of the landing and buffering process of airborne armored vehicle under typical airdrop conditions, an analysis was conducted towards the cumulative damage evaluation for the structure of airborne armored vehicle in repeated airdrop. Conclusions are obtained as follows: 1) when the vertical landing speed is lower than 8m/s over a plain, the structures stress in the vehicle would not exceed the yield limit of materials, thus no damage would be caused to the vehicle structure. Therefore, the airborne armored vehicle is secure in repeated airdrop under normal conditions; 2) Three times of airdrop can be executed at most for airborne armored vehicle when the vertical landing speed is 9m/s; 3) In repeated landing under the same airdrop conditions, increase of the value of structural damage is non-linear.

5. References

[1] Li Jian-yang, Wang Hong-yan, Rui Qiang, Hong Huang-jie, Zhang Fang. Research on Cumulative Damage Assessment Method for Airborne Vehicle at Landing Based on Finite Element Analysis [J]. Journal of System Simulation, 2014.1, 26(1)pp 208-214

[2] Li Jian-yang, Wang Hong-yan, Hao Gui-xiang. Simulation of Landing Process Based on Explicit Finite Element Method [J]. Journal of Academy of Armored Force Engineering, 2010.6, 24(3)pp 25-28

[3] J Lemaitre. A continuous damage mechanics model for ductile fracture[J]. Journal of Engineering Materials and Technology, Transactions of the ASME (s0094-4289), 1985, 107(1) pp 83-89

[4] LI Yun-fei, Zeng Xiang-guo, Liao Yi. Thermal-viscoplastic constitutive relation of Ti-6A1-4V alloy and numerical simulation by modified Johnson-Cook modal [J]. The Chinese Journal of Nonferrous Metals, 2017.7, 27(7)pp 1419-1425